International Journal of Mass Spectrometry 276 (2008) 153–159

Contents lists available at ScienceDirect

International Journal of Mass Spectrometry

journal homepage: www.elsevier.com/locate/ijms

Proton hydrates as soft ion/ion proton transfer reagents for multiply deprotonated biomolecules

Jeremiah J. Bowers[a], Brittany D.M. Hodges[a], Ola M. Saad[b,1], Julie A. Leary[b], Scott A. McLuckey[a,*]

[a] Department of Chemistry, Purdue University, 560 Oval Drive, West Lafayette, IN 47907-2084, United States
[b] Genome Center, Departments of Chemistry and Molecular Cell Biology, University of California, Davis, CA 95616, United States

ARTICLE INFO

Article history:
Received 16 April 2008
Received in revised form 23 May 2008
Accepted 27 May 2008
Available online 3 June 2008

Keywords:
Ion/ion reaction
Sulfated oligosaccharide anion
Proton hydrates
Quadrupole ion trap

ABSTRACT

Ion/ion proton transfer from protonated strong gaseous bases such as pyridine and 1,8-bis(dimethylamino)naphthalene (i.e., the proton sponge), to multiply charged anions derived from a sulfated pentasaccharide drug, Arixtra™, gives rise to extensive fragmentation of the oligosaccharide. This drug serves as a model for sulfated glycosaminoglycans, an important class of polymers in glycobiology. The extent of fragmentation appears to correlate with the proton affinity of the molecule used to transfer the proton, which in turn correlates with the reaction exothermicity. Consistent with tandem mass spectrometry results, anions with sodium counter-ions are more stable with respect to fragmentation under ion/ion proton transfer conditions than ions of the same charge state with protons counter-ions. Proton hydrates were found to give rise to much less anion fragmentation and constitute the softest protonation agents thus far identified for manipulating the charge states of multiply charged biopolymer anions. The reaction exothermicities associated with proton hydrates comprised of five or more water molecules are lower than that for protonated proton sponge, which is among the softest reagents thus far examined for ion/ion proton transfer reactions. The partitioning of ion/ion reaction exothermicity among all of the degrees of freedom of the products may also differ for proton hydrates relative to protonated molecules. However, a difference in energy partitioning need not be invoked to rationalize the results reported here.

1. Introduction

The gas-phase manipulation of the charge states of multiply charged ions formed via spray ionization has been effected with ion/molecule [1–4] and ion/ion reactions [5–8]. Generating conditions for efficient ion/ion reactions is generally more demanding from the instrumentation standpoint than it is for ion/molecule reactions. However, ion/ion reactions have been demonstrated to be more effective than ion/molecule reactions in reducing charge states to arbitrarily low values. Ion/ion reactions have also proved to be more universal than ion/molecule reactions due to the relatively high exothermicities associated with essentially all reactions of oppositely charged ions and reaction kinetics that are largely independent of the chemical nature of the reactants [9]. It is also generally easier to control the timing and location of ion/ion reactions because both reactants can be manipulated with external fields. The unique characteristics of ion/ion reactions, therefore, underlie a number of applications for charge state manipulation. For example, ion/ion reactions have been used to facilitate the determination of charge states [10], the simplification of electrospray mass spectra of mixtures of polymers such as proteins [11,12], oligonucleotides [13], and synthetic polymers [14], the simplification of product ion spectra in tandem mass spectrometry [15], and for concentrating ions initially formed over a range of charge states into one or a few charge states [16,17].

While in some applications of ion/ion reactions, such as electron transfer dissociation [18], it is desirable to induce fragmentation; for most charge state manipulation applications, it is desirable to avoid fragmentation of the analyte ion. As a result of the relatively high potential energies associated with the reactions of ions of opposite polarity, a number of product ion channels are accessible in principle, including the fragmentation of one or both of the reactants. The likelihood for fragmentation of an ion/ion reaction product is dependent upon the reaction exothermicity, the partitioning of the reaction exothermicity among translational and internal degrees of freedom of the products, as well as the kinetic stabilities of the products. The lifetimes of excited ion/ion reaction products, for example, are particularly important in determining the extent of fragmentation in the ion trap environment as removal of excess energy via collisions with the bath gas and/or IR emission

* Corresponding author. Tel.: +1 765 494 5270; fax: +1 765 494 0239.
E-mail address: mcluckey@purdue.edu (S.A. McLuckey).
[1] Current address: BioAnalytical Research & Development, Genentech, Inc., 1 DNA Way, South San Francisco, CA 94080-4990, United States.

1387-3806/$ – see front matter © 2008 Elsevier B.V. All rights reserved.
doi:10.1016/j.ijms.2008.05.038

can compete with dissociation [19,20]. Hence, in the case of electron transfer from oligonucleotide anions, it has been noted that fragmentation decreases as the number of residues in the oligonucleotide anion increases [21], which is consistent with increasing ion lifetime with numbers of degrees of freedom. In the case of deprotonation of multiply protonated peptides or proteins, fragmentation of the cationic products from ion/ion reactions has not been observed, even for non-covalently bound complexes [22]. On the other hand, evidence for a minor degree of fragmentation of 5′-d(AAAA)-3′oligonucleotide anions upon reaction of the triply deprotonated species, $[M-3H]^{3-}$, with protonated isobutylene ($C_4H_9^+$) has been noted [23]. Protonation of the same anions using either protonated pyridine [24] or protonated benzoquinoline [23], showed no measurable fragmentation. This result is consistent with reaction exothermicity in that isobutene has a significantly lower proton affinity than either pyridine or benzoquinoline. Very little fragmentation of anions derived from 5′d$(A)_{20}$-3′ was noted upon protonation with $C_4H_9^+$ [23], which is consistent with the decrease in fragmentation noted in electron transfer ion/ion reactions as the number of residues increased.

Protonated reagents with relatively high proton affinities can be used to manipulate the charge states of oligonucleotide anions with inconsequential degrees of fragmentation. However, in exploring the ion/ion charge state manipulation of multiply charged anions derived from sulfated glycosaminoglycans (GAGs) we have found that extensive fragmentation of the anions follows from reactions with even the softest proton transfer reagents developed for the charge state manipulation of oligonucleotide anions. Sulfated or heparin-like GAGs play important roles in glycobiology and there is a need for structural characterization tools to address the structural diversity of this class of biopolymer. For this reason, tandem mass spectrometry has been applied to ions derived from sulfated GAGs [25–30]. The charge states and counter-ion identities of the ions have been shown to be important factors in determining the favored dissociation channels in tandem mass spectrometry. It is therefore of interest to be able to manipulate charge states and counter-ion identities via ion/ion reaction techniques, as has been demonstrated to be possible with other types of biopolymers. In this work, we describe results for ion/ion reactions involving absolute charge state reduction of anions derived from the electrospray ionization of Fondaparinux (Arixtra™), an octasulfated pentasaccharide anticoagulant drug.

2. Experimental methods

2.1. Materials

Fondaparinux (Arixtra™) (methyl-*O*-2-deoxy-6-*O*-sulfo-2-(sulfoamino)-*R*-D-glucopyranosyl-(1 → 4)-*O*-*β*-D-glucopyranuronosyl-(1 → 4)-*O*-2-deoxy-3,6-di-*O*-sulfo-2-(sulfoamino)-α-D-glucopyranosyl-(1 → 4)-*O*-2-*O*-sulfo-α-L-idopyranuronosyl-(1 → 4)-2-deoxy-6-*O*-sulfo-2-(sulfoamino)-α-D-glucopyranoside) sodium chloride solution was obtained from Synofi-Synthelabo, which was lyophilized and then desalted using a 1000 molecular weight cut-off SpinCon dialyzer. The reconstituted sample was then diluted to 0.1 mM in water from which a 10 μM buffer solution of water: ammonium hydroxide (98:2) was prepared for negative electrospray. The reagents 7,8-benzoquinoline, 1,8-bis(dimethylamino)naphthalene, and pyridine were all purchased from Sigma–Aldrich (St. Louis, MO). Solutions of 7,8-benzoquinoline and 1,8-bis(dimethylamino)naphthalene were prepared at concentrations of 1 mg/mL with solutions of 1% acetic acid in water and water:methanol:acetic acid (79.5:19.5:1), respectively. A 1% acetic acid in water solution was used to generate proton hydrate clusters. Protonated pyridine was generated by atmospheric sampling glow discharge ionization (ASGDI) [31].

2.2. Procedures

Most experiments were performed using a Finnigan Ion Trap Mass Spectrometer (ITMS) (San Jose, CA) equipped with two ion sources described in detail previously [32]. A DC turning quadrupole is used to direct the sequential injection of ions from two ion sources through the ion trap end-cap electrode. The injection and timing of all sources are controlled by the ITMS software. Nanoelectrospray emitters were used for generating anions and cations, except for pyridine which was generated via ASGDI. Borosilicate glass capillaries (0.86 mm i.d., 1.5 mm o.d.) were pulled using a P-87 Flaming/Brown micropipet puller (Sutter Instruments, Novato, CA) to form nanoelectrospray emitters. Anions formed from Fondaparinux were accumulated for 0.5–0.9 s followed by ion isolation steps performed by using radio frequency (rf) ion isolation ramps tuned to eject ions of selected mass-to-charge ratios [33]. Cations derived from the strong bases were subsequently injected for 50–300 ms. Fondaparinux anions were then allowed to undergo proton transfer reactions for 100–500 ms after which anion product ion spectra were obtained via resonance ejection [34]. For proton hydrate ion/ion reactions with Arixtra™ anions, the reactions took place during the cation injection period. Calibration of the product ion spectra was accomplished by using the charge states formed from the nanoelectrospray of a mixture of α-D-Glucose-1-phosphate, GAILDGAILR, and Bombesin.

Experiments involving proton hydrates and Fondaparinux were performed on a Finnigan ITMS equipped with up to four ion sources modified for ion–ion reactions described previously [35]. However, in this report only two ion sources were used for ion injection through the end-cap electrode of the ion trap. The order of events in these experiments was identical to those outlined above. One

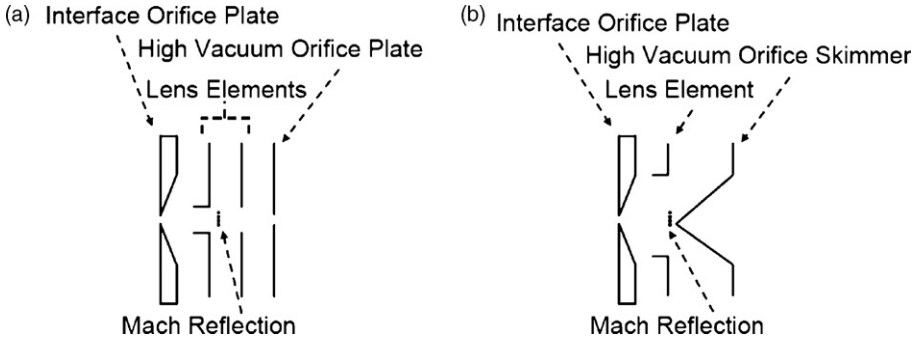

Fig. 1. Schematic diagrams of two atmosphere/vacuum interface/lens arrangements. (a) Interface designed to sample largely desolvated ions in which the aperture into the high vacuum region is situated 6.49 mm after the mach reflection. (b) An interface that samples cluster ions via a skimmer cone situated 0.49 mm after the mach reflection.

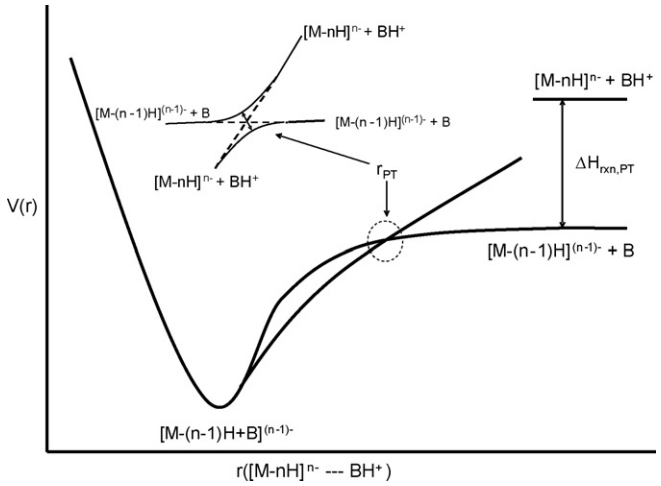

Fig. 2. Generalized energy diagram for a single proton transfer reaction involving a multiply deprotonated species of interest, $(M-nH)^{n-}$, and a protonated base, BH^+.

of the atmosphere/vacuum interfaces, both of which are shown schematically in Fig. 1, was modified to maximize cluster formation and transmission through the interface by sampling ions 0.49 mm beyond the mach disk via a skimmer cone rather than 6.49 mm beyond the mach disk via an orifice in a flat plate in the original source design.

3. Results and discussion

A generalized energy diagram for the single proton transfer from a protonated reagent species to a multiply deprotonated molecule of interest is shown in Fig. 2. The entrance channel, depicted on the left, is characterized by the long range $1/r$ attraction associated with oppositely charged ions. The exit channel shown on the right proceeds over an ion/neutral surface, such as that ordinarily encountered in ion/molecule reactions. The reaction enthalpy is given by the following relation

$$\Delta H_{\mathrm{rxn}} = \mathrm{PA[B]} - \mathrm{PA}[(\mathrm{M}-n\mathrm{H})^{n-}] \quad (1)$$

where the proton affinity of the multiply deprotonated species is given by $\mathrm{PA}[(\mathrm{M}-n\mathrm{H})^{n-}]$ and the proton affinity of the conjugate base of the singly protonated species is denoted as PA[B].

It is clear from relation (1) and Fig. 2 that the energy available for partitioning into product ions can be varied by changing either the proton affinity of the reagent B or the proton affinity of the multiply charged anion (via charge state). Reagent molecules of high proton affinity and anions of relatively low charge minimize the reaction exothermicity.

Ion/ion proton transfer reactions involving multiply charged reactants have shown evidence for proton transfer via a long-lived intermediate complex (i.e., a complex that survives for many vibrational periods) and at points on the energy surface where reactant and product states cross [36]. The latter process can occur during the time of passage of the reactants through the distance of separation associated with the crossing point and need not involve the formation of a long-lived complex. The different possible reaction dynamics are relevant with respect to energy partitioning among the various degrees of freedom of the products, both internal and translational, because energy partitioning may differ if proton transfer occurs largely via a long-lived complex or via a crossing on the energy surface as the reactants pass one another.

The results described below summarize observations made in proton transfer reactions to anions derived from the sulfated pentasaccharide Fondaparinux (Arixtra™), the structure of which (with protons as counter-ions) is shown in Scheme 1.

The molecule has eight sulfate groups and two carboxylate groups and, as a result, tends to form multiply charged anions upon electrospray ionization. The ion/ion proton transfer behavior of these ions is dependent upon the proton affinity of the neutral species used to form the cationic reagent, the charge state of the anion, and the extent to which protons are replaced by sodium ions, as illustrated below. Fig. 3 compares the negative product ion spectra resulting from the reaction of the $[M-5H]^{5-}$ ion of Arixtra™ with (a) protonated pyridine (PY), (b) protonated 7,8-benzoquinoline (BQ), and protonated 1,8-bis(dimethylamino)naphthalene, commonly known as 'proton sponge' (PS). The proton affinities of these compounds are 930 kJ/mol [37], 961 kJ/mol [23], and 1028 kJ/mol [37], respectively. All of these reagents are relatively basic, with the proton sponge

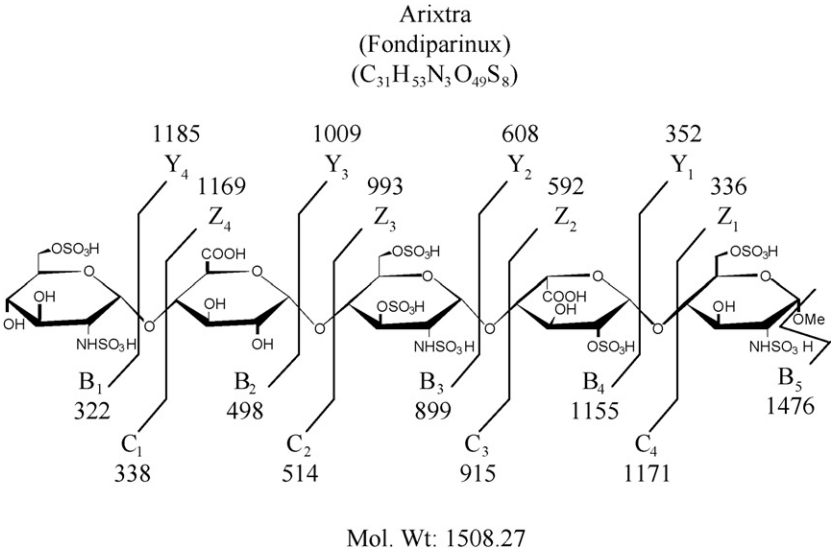

Scheme 1. Structure of Arixtra™ showing major product ions that arise from intersaccharide cleavages.

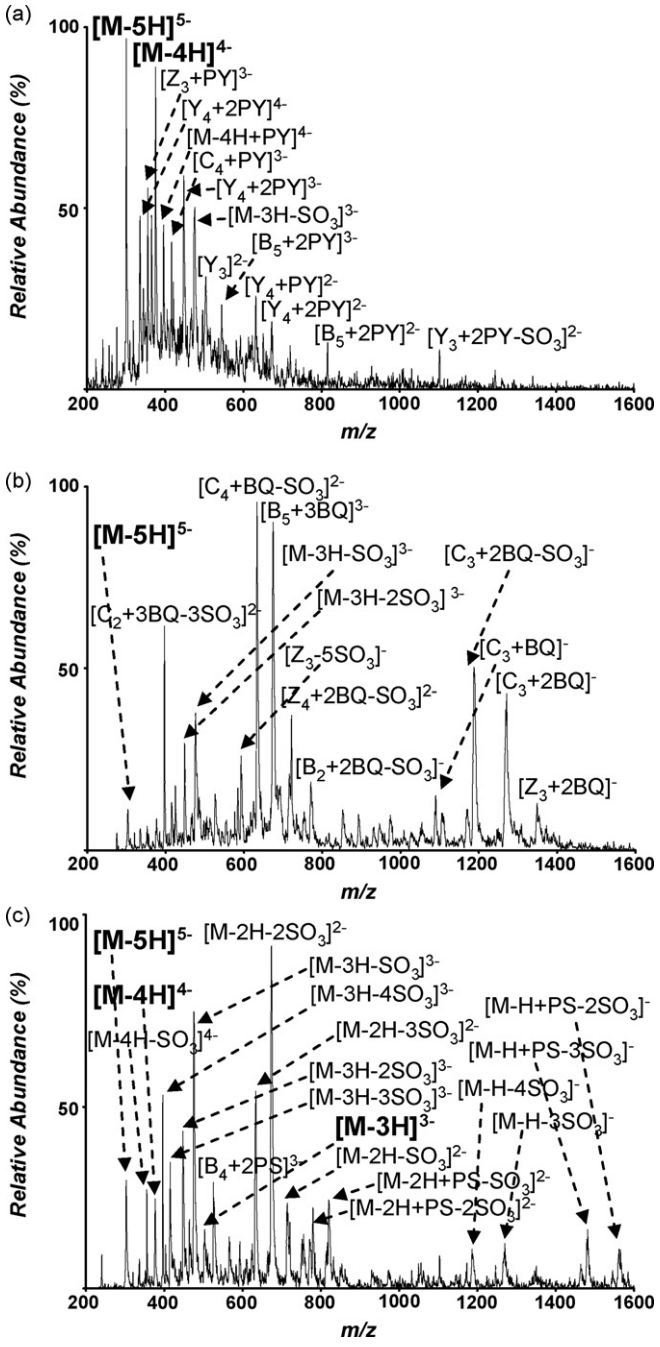

Fig. 3. Negative ion product spectra from the reaction of the $[M-5H]^{5-}$ ion of Arixtra™ with (a) protonated pyridine (PY), (b) protonated benzoquinoline (BQ), and (c) protonated proton sponge (PS).

being among the most basic neutral molecules for which a proton affinity has been measured.

Protonated versions of each of these reagents also tend to react with multiply charged oligonucleotide anions without giving rise to significant fragmentation. No fragmentation has been noted for ion/ion reactions of oligonucleotide anions with protonated BQ or protonated PS. In contrast, all of the reagent cations formed from these basic molecules give rise to extensive fragmentation of the Arixtra™ $[M-5H]^{5-}$ ion upon ion/ion reaction. Furthermore, each of the reagent cations shows a tendency for attachment to the Arixtra™ product anions (primarily to fragment ions that arise from intersaccharide cleavages). Under the reaction conditions used to collect the data in Fig. 3, consecutive ion/ion reactions could occur such that a mixture of products that result from attachment in the first reaction step, or in subsequent reaction steps with first generation products ions, or a combination thereof, contribute to the data. It is not surprising to observe cation attachment to these anions because previous studies have shown that the charged sulfate functionality can give rise to relatively stable interactions with protonated strong bases [38]. The observation of the adduct ions is significant in that it indicates that, at a minimum, a substantial fraction of the reactions take place through a long-lived complex. The nature of the fragmentation observed with these reagents qualitatively appears to be consistent with the order of the reagent proton affinities. For example, the reagents with the lower proton affinities, which correlates with higher reaction exothermicies (see relation (1)), show both losses of SO_3 and interresidue cleavages. The loss of SO_3 is known from CID experiments to be favored over interresidue cleavages when a proton counter-ion to the sulfate is present [39]. Regardless of the presence or absence of a proton counter-ion in the Arixtra™ reactant, the ion/ion reaction product is expected to be comprised of at least one protonated sulfate group as a result of the use of a proton transfer reagent cation. The appearance of both sulfate loss(es) and interresidue cleavages in the post-ion/ion reaction data with protonated pyridine and protonated benzoquinoline suggests that sufficient energy is available to make interresidue cleavages competitive either as first generation or subsequent generation cleavages. While protonated proton sponge also gives rise to extensive fragmentation, relatively little interresidue cleavage is noted.

The exothermicity of a singly charged cation/multiply charged anion proton transfer reaction increases with the charge of the multiply charged reactant due to the role of the electrostatic potential on the proton affinity of the anion. The results of Fig. 4, which shows anionic product ion data for the reactions of the $[M-6H]^{6-}$ and $[M-4H]^{4-}$ anions in reaction with protonated benzoquinoline, along with the data of Fig. 3b for the corresponding reaction with the $[M-5H]^{5-}$ anion, illustrate the role of Arixtra™ anion charge.

It is clear from comparing the data for the three Arixtra™ charge states (Figs. 4 and 3b) that significantly greater degrees of fragmentation, including major contributions from interresidue cleavages, are noted as the absolute anion charge state increases. These observations are consistent with those obtained via charge state dependent collision-induced dissociation [27]. In the case of the $[M-4H]^{4-}$ ion, there is even evidence for the formation of a singly charged ion with the loss of only one molecule of SO_3, although the abundance of this product is quite small. Nevertheless, it represents three sequential ion/ion proton transfer reactions that result in only one apparent cleavage. As noted in Fig. 3, benzoquinoline attaches to interresidue cleavage products more than to SO_3 loss products. It is not clear from these data why reagent cation attachment to SO_3 loss products is not more prominent. However, the rearrangement mechanism associated with SO_3 loss from a protonated sulfate group may either be inhibited by the presence of an attached base molecule, or binding of the base molecule to the hydroxyl group on the Arixtra™ ion that is formed by SO_3 loss may be weak (i.e., the interaction that stabilizes the adduct is destroyed when SO_3 is lost and the adduct is therefore lost along with SO_3).

The kinetic stabilities of sulfated oligosaccharide anions are also influenced by the nature of the counter-ion associated with the sulfate groups. The facile rearrangement associated with SO_3 loss from sulfate groups with proton counter-ions is inhibited with metal counter-ions, such as the sodium ion [27]. This behavior is also reflected in the ion/ion reactions involving Arixtra™ anions with various numbers of sodium counter-ions, which are readily formed under conditions in which de-salting is minimized. Fig. 5 illustrates the ion/ion reaction tendencies noted for Arixtra™ anions with

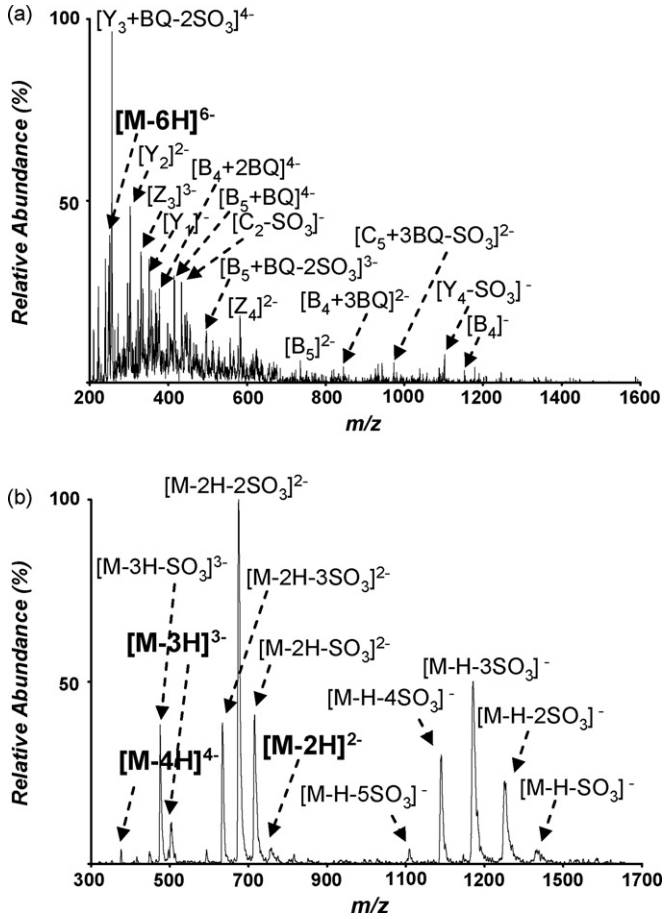

Fig. 4. Negative ion product spectra from the reaction of protonated benzoquinoline (BQ) with (a) the $[M-6H]^{6-}$ ion of Arixtra™ and (b) with the $[M-4H]^{4-}$ anion of Arixtra™.

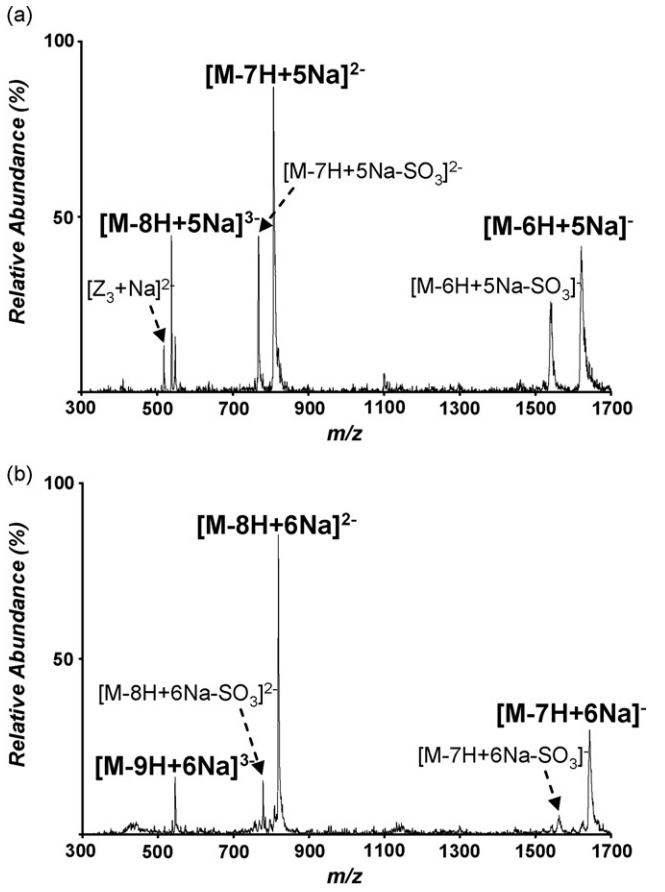

Fig. 5. Negative ion product spectra from the reaction of protonated benzoquinoline with (a) the $[M-9H+5Na]^{4-}$ ion of Arixtra™ and (b) with the $[M-10H+6Na]^{4-}$ anion of Arixtra™.

sodium counter-ions and protonated strong bases. Fig. 5a shows the negative product ion spectrum for the $[M-9H+5Na]^{4-}$ anions in reaction with protonated benzoquinoline while Fig. 5b shows the results for the reaction with the $[M-10H+6Na]^{4-}$ anion.

Consistent with collision-induced dissociation results [40–42] the sodium counter-ion containing anions appear to be more stable with respect to fragmentation than the proton counter-ion-only anions of the same charge state. (Compare Fig. 5 data with Fig. 4b, for example.)

All of the ion/ion reaction data involving protonated strong bases as cationic reagents are consistent with the extent of observed fragmentation of Arixtra™ anions being related to the ion/ion reaction exothermicity. Fragmentation tends to increase with anion charge state and to decrease with increasing proton affinity of the reagent molecule used to form the cationic reagent. Even with one of the most basic reagents available, however, it was not possible to protonate the non-metal-containing Arixtra™ anions via ion/ion reaction without inducing extensive fragmentation. For this reason, we chose to explore the possibility for charge state manipulation using cluster ions, specifically proton hydrates. The use of proton hydrates as protonating reagents has two potential advantages over the use of a single protonated molecule: (i) stabilization of the proton by clustering can lower the effective proton affinity of the reagent cation and (ii) if the reaction proceeds via a long-lived complex, excess reaction exothermicity can be partitioned into translational (and internal) modes of individual water molecules as the long-lived complex breaks-up. In the latter scenario, the weakly bound nature of the reagent cation as it collides with the anion provides many low energy dissociation channels leading to liberation of individual water molecules that can carry off excess energy.

The lifetimes of proton hydrates, $(H_2O)_xH^+$, of $n > 6$ in the room temperature ion trap with a background pressure of helium of the order of 1 mTorr are generally less than roughly 10 ms [43]. The scan time for an ion trap is on the order of tens of milliseconds. For this reason, it is difficult to determine the distribution of proton hydrates that enter the ion trap due to the rapid decomposition of the higher cluster sizes on the time frame of the experiment. Fig. 6 shows a nanoelectrospray mass spectrum of a 1% aqueous acetic acid solution acquired immediately after a cation accumulation period via the interface of Fig. 1a. The large ill-defined baseline upon which discrete cluster ions are apparent in Fig. 6 is symptomatic of ions fragmenting during the scan. When delay periods were introduced after the ion accumulation step and prior to mass analysis, the broad baseline largely disappeared and the resulting mass spectra (data not shown) exhibited major shifts to smaller cluster sizes ($x < 10$). These observations indicate that the proton hydrate distribution that is initially injected into the ion trap consists of significantly larger proton hydrates than those shown in Fig. 6. The ion/ion reaction experiments involving the proton hydrates were conducted under conditions in which the stored Arixtra™ anion population was exposed continuously to proton hydrates being injected into the ion trap along with those that evolved from larger clusters during the ion/ion reaction period. For example, a large proton hydrate captured early in the ion/ion reaction period might

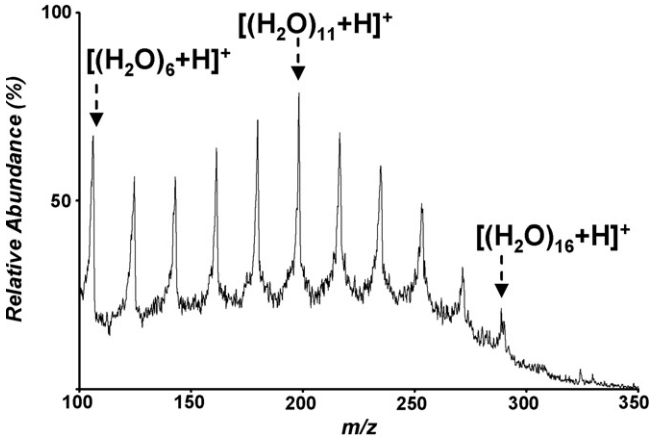

Fig. 6. Nanoelectrospray mass spectrum of a 1% acetic acid in water solution with minimal delay time between the end of ion accumulation and the beginning of the mass scan.

undergo significant desolvation before it encounters an Arixtra^{TM} anion. Hence, the cationic reagent population is expected to be comprised of a very large range of cluster sizes. The continuous positive reagent accumulation approach was used to maximize the likelihood for reactions with larger cluster sizes, which lead to reactions of lower enthalpy (see below).

Fig. 7 shows the post-ion/ion reaction negative ion spectra resulting from the reaction of the proton hydrate mixture with the $[M-6H]^{6-}$ (Fig. 7a), $[M-5H]^{5-}$ (Fig. 7b), and $[M-4H]^{4-}$ (Fig. 7c) anions of Arixtra^{TM}. It is clear in all cases that far more proton transfer without dissociation takes place with the proton hydrate mixture than with any of the protonated strong bases (see Figs. 3 and 4 for direct comparisons).

In the case of the $[M-6H]^{6-}$ ion, evidence for $[M-7H+Na]^{6-}$ and $[M-8H+2Na]^{6-}$ ions in the isolated reactant anion population was apparent, along with ions of slightly lower mass (see the insert of Fig. 7(a)). The sodium containing ions as well as an ion indicated as being Arixtra^{TM} that is deficient by one water molecule are apparent in the charge-reduced products. It is not clear whether or not the lower mass ion is a fragment that arises due to the ion/ion reaction. Water loss, for example, is not a major process noted for these ions. Rather, it is likely that it is a charge-reduced version of the low mass shoulder in the isolated ion population. There is evidence for minor products due to SO_3 loss and these are likely due to ion/ion proton transfer. In the case of the $[M-5H]^{5-}$ ion, proton transfer without fragmentation is clearly the most prominent process and there is a small degree of loss of SO_3 associated with the $[M-3H]^{3-}$ product, which is formed via sequential proton transfer. Many of the other peaks in the spectrum do not correspond to fragments that can be readily rationalized as arising from Arixtra^{TM}. It is possible that at least some of these signals may arise from chemical noise present in the isolated ion population. The observation that little fragmentation is noted for the reactions of the $[M-6H]^{6-}$ ion is another piece of evidence that the unidentified peaks in Fig. 7(b) do not arise from fragmentation induced by the ion/ion reactions. Very little fragmentation is associated with proton transfer to the $[M-4H]^{4-}$ ion, which stands in contrast with the results for protonated BQ (Fig. 4b). Note that the results shown here show charge state reduction to $[M-3H]^{3-}$ using proton hydrates but further charge state reduction can also be effected. Each subsequent proton transfer reaction is less likely to result in fragmentation due to the increasing kinetic stability of the Arixtra anions due to reduction in intramolecular electrostatic repulsion and to lower heats of reaction for the ion/ion reactions.

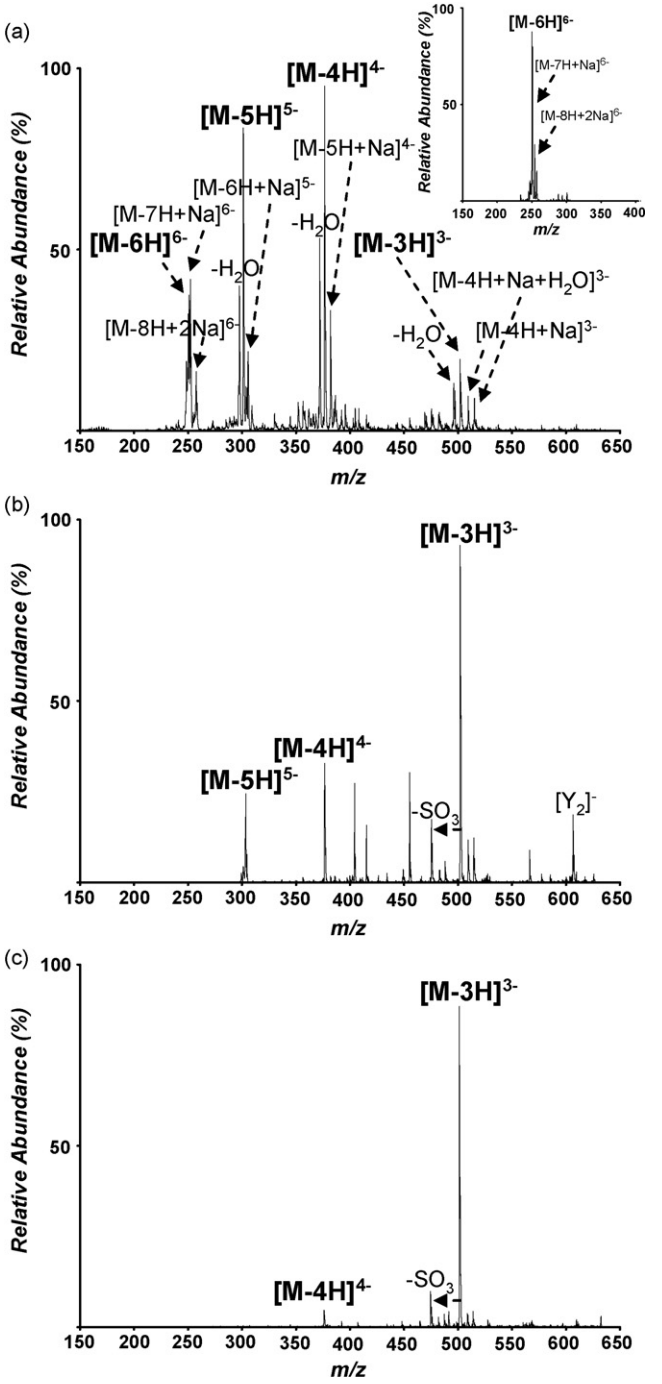

Fig. 7. Negative ion product spectra from the reactions of continuously accumulated proton hydrates with stored (a) $[M-6H]^{6-}$, (b) $[M-5H]^{5-}$, and (c) $[M-4H]^{4-}$ anions of Arixtra^{TM}.

The post-ion–ion product ion spectra shown in Fig. 7 show that proton hydrates are far more effective in transferring protons to Arixtra^{TM} without giving rise to fragmentation than even the protonated proton sponge. While a difference in the partitioning of reaction exothermicity might play a role in the observed differences in Arixtra^{TM} anion fragmentation resulting from proton transfer from proton hydrates versus protonated strong bases cannot be precluded, there is also a significantly lower reaction exothermicity associated with proton transfer from the proton hydrates. Hence, the lower extent of fragmentation may simply arise from lower ion/ion reaction exothermicities. The net reaction for any given pro-

ton hydrate, $(H_2O)_xH^+$, with a multiply deprotonated molecule is given by

$$[M-nH]^{n-} + (H_2O)_xH^+ \rightarrow [M-(n+1)H]^{(n-1)-} + xH_2O \quad (2)$$

In contrast with the use of singly protonated molecules, the proton affinity term in relation (1) applies to a case in which the proton is solvated by multiple molecules. In the case of a proton hydrate, the relevant value for use in relation (1) is the negative of the enthalpy change associated with reaction (3):

$$xH_2O + H^+ \rightarrow (H_2O)_xH^+ \quad (3)$$

This value can be estimated by summing the individual ΔH values associated with the step-wise solvation of the proton [44–47]. For example, the enthalpies associated with the step-wise solvation of the proton to form the $(H_2O)_8H^+$ ion [48] sum to −1175 kJ/mol, which is well in excess of the enthalpy associated with protonation of the proton sponge. The bulk condensation energy of water is roughly −44 kJ/mol so that proton transfer reactions involving the larger proton hydrates are expected to be even less exothermic. In fact, at some point the proton transfer reaction can become endothermic. However, at room temperature in the ion trap, any proton hydrate that might be involved in a long-lived complex with an Arixtra™ anion will desolvate to the point at which proton transfer becomes exothermic. In any case, it is clear that proton hydrates are much "softer" reagents for proton transfer to anions than are protonated strong neutral bases, such as the proton sponge. The dissociation of the cluster ion from a long-lived ion/ion reaction complex can also minimize energy deposition into the Arixtra™ anion. Hence, cluster ions as ion/ion reaction reagents may open additional channels for the partitioning of reaction exothermicity. However, it is unclear to what extent this possibility may contribute to the data reported here because the lower reaction exothermicity alone may account for the minimal degree of fragmentation associated with proton transfer from the proton hydrates.

4. Conclusions

Multiply charged anions of the sulfated pentasaccharide drug Arixtra™ show extensive fragmentation upon protonation by protonated pyridine, protonated 7,8-benzoquinoline, and protonated 1,8-bis(dimethylamino)naphthalene. The extent of fragmentation correlates with the proton affinity of the molecule and the charge state of the anion, which correlate in turn with the exothermicity of the reaction. These protonated molecules have been shown to be effective in protonating multiply charged anions of oligonucleotides without giving rise to fragmentation. The Arixtra™ anions, therefore, are particularly sensitive indicators of ion/ion reaction exothermicity. Proton hydrates, on the other hand, give rise to much less fragmentation of Arixtra™ anions upon proton transfer. Due to the high dissociation rates of proton hydrates in the room temperature ion trap environment, the ion/ion reactions with proton hydrates were conducted by storing the anions while exposing them to cations that were continuously accumulated in the ion trap. The cationic reactants, therefore, were comprised of a wide range of proton hydrates with some of the reactants likely to consist of well over a dozen water molecules. The reaction exothermicities of proton transfer from the larger proton hydrates ($n > 6$) are significantly smaller than those associated with the reactions of the protonated strong bases mentioned above. This alone may account for the lesser degree of fragmentation associated with proton transfer from the proton hydrates. The use of cluster ions as proton transfer reagents may also result in differences in the partitioning of ion/ion reaction exothermicity due to the possibility for water loss from a long-lived ion/ion reaction intermediate. Differences in energy partitioning, however, need not be invoked in this case to account for the lesser degrees of fragmentation associated with the proton hydrates.

Acknowledgment

This work was supported by the Office of Basic Energy Sciences, Division of Chemical Sciences under Award No. DE-FG02-00ER15105.

References

[1] S.A. McLuckey, G.J. Van Berkel, G.L. Glish, J. Am. Chem. Soc. 112 (1990) 5668.
[2] S.A. McLuckey, G.L. Glish, G.J. Van Berkel, Anal. Chem. 63 (1991) 1971.
[3] E.R. Williams, J. Mass Spectrom. 31 (1996) 831.
[4] J.D. Lennon, S.P. Cole, G.L. Glish, Anal. Chem. 78 (2006) 8472.
[5] J.L. Stephenson Jr., S.A. McLuckey, J. Am. Chem. Soc. 118 (1996) 7390.
[6] M. Scalf, M.S. Westphall, J. Krause, S.L. Kaufman, L.M. Smith, Science 283 (1999) 194.
[7] S.A. McLuckey, J.L. Stephenson Jr., Mass Spectrom. Rev. 17 (1998) 369.
[8] S.J. Pitteri, S.A. McLuckey, Mass Spectrom. Rev. 24 (2005) 931.
[9] S.A. McLuckey, J.L. Stephenson Jr., K.G. Asano, Anal. Chem. 70 (1998) 1198.
[10] W.J. Herron, D.E. Goeringer, S.A. McLuckey, Anal. Chem. 68 (1996) 257.
[11] J.L. Stephenson Jr., S.A. McLuckey, Anal. Chem. 68 (1996) 4026.
[12] M. Scalf, M.S. Westphall, L.M. Smith, Anal. Chem. 72 (2000) 52.
[13] S.A. McLuckey, J. Wu, J.L. Bundy, J.L. Stephenson Jr., G.B. Hurst, Anal. Chem. 74 (2002) 976.
[14] J.L. Stephenson Jr., S.A. McLuckey, J. Am. Soc. Mass Spectrom. 9 (1998) 957.
[15] J.L. Stephenson Jr., S.A. McLuckey, Anal. Chem. 70 (1998) 3533.
[16] S.A. McLuckey, G.E. Reid, J.M. Wells, Anal. Chem. 74 (2002) 336.
[17] P.A. Chrisman, S.J. Pitteri, S.A. McLuckey, Anal. Chem. 78 (2006) 310.
[18] J.E.P. Syka, J.J. Coon, M.J. Schroeder, J. Shabanowitz, D.F. Hunt, Proc. Natl. Acad. Sci. U.S.A. 101 (2004) 9528.
[19] D.E. Goeringer, S.A. McLuckey, Int. J. Mass Spectrom. 177 (1998) 163.
[20] D.M. Black, A.H. Payne, G.L. Glish, J. Am. Soc. Mass Spectrom. 7 (2006) 932.
[21] J.L. Stephenson Jr., S.A. McLuckey, Rapid Commun. Mass Spectrom. 11 (1997) 875.
[22] J.L. Stephenson Jr., G.J. Van Berkel, S.A. McLuckey, J. Am. Soc. Mass Spectrom. 8 (1997) 637.
[23] J. Wu, S.A. McLuckey, Int. J. Mass Spectrom. 228 (2003) 577.
[24] W.J. Herron, D.E. Goeringer, S.A. McLuckey, J. Am. Soc. Mass Spectrom. 6 (1995) 529.
[25] H. Desaire, T.L. Sirich, J.A. Leary, Anal. Chem. 73 (2001) 3513.
[26] H. Desaire, J.A. Leary, J. Am. Soc. Mass Spectrom. 11 (2000) 916.
[27] J. Zaia, C.E. Costello, Anal. Chem. 75 (2003) 2445.
[28] J.J. Wolff, I.J. Amster, L.L. Chi, R.J. Linhardt, J. Am. Soc. Mass Spectrom. 18 (2007) 234.
[29] N.G. Karlsson, H. Karlsson, G.C. Hansson, J. Mass Spectrom. 31 (1996) 560.
[30] O.M. Saad, J.A. Leary, Anal. Chem. 75 (2003) 2985.
[31] S.A. McLuckey, G.L. Glish, K.G. Asano, B.C. Grant, Anal. Chem. 60 (1988) 2220.
[32] J.M. Wells, P.A. Chrisman, S.A. McLuckey, J. Am. Soc. Mass Spectrom. 13 (2002) 614.
[33] S.A. McLuckey, D.E. Goeringer, G.L. Glish, J. Am. Soc. Mass Spectrom. 2 (1991) 11.
[34] R.E. Kaiser, R.G. Cooks, G.C. Stafford, J.E.P. Syka, P.H. Hemberger, Int. J. Mass Spectrom. Ion Process. 106 (1991) 79.
[35] E.R. Badman, P.A. Chrisman, S.A. McLuckey, Anal. Chem. 74 (2002) 6237.
[36] J.M. Wells, P.A. Chrisman, S.A. McLuckey, J. Am. Chem. Soc. 125 (2003) 7238.
[37] E.P. Hunter, S.G. Lias, Proton Affinity Evaluation in NIST Chemistry WebBook, NIST Standard Reference Database Number 69, in: P.J. Linstrom, W.G. Mallard (Eds.), June 2005, National Institute of Standards and Technology, Gaithersburg MD, 20899 (http://www.webbook.nist.gov).
[38] M. He, J.F. Emory, S.A. McLuckey, Anal. Chem. 77 (2005) 3173.
[39] J.M. McClellan, C.E. Costello, P.B. O'Connor, J. Zaia, Anal. Chem. 74 (2002) 3760.
[40] J. Zaia, Mass Spectrom. Rev. 23 (2004) 161.
[41] M.T. Cancilla, S.G. Penn, J.A. Carroll, C.E. Lebrilla, J. Am. Chem. Soc. 118 (1996) 6736.
[42] R. Orlando, C.A. Bush, C. Fenselau, Biomed. Environ. Mass Spectrom. 19 (1990) 747.
[43] S.A. McLuckey, G.L. Glish, K.G. Asano, J.E. Bartmess, Int. J. Mass Spectrom. Ion Process. 109 (1991) 171.
[44] M. Meot-Ner, Chem. Rev. 105 (2005) 213.
[45] A.J. Cunningham, A.J. Payzant, P. Kebarle, J. Am. Chem. Soc. 94 (1972) 7627.
[46] Y.K. Lau, S. Ikuta, P. Kebarle, J. Am. Chem. Soc. 104 (1982) 1462.
[47] R. Kelterbaum, E. Kochanski, J. Phys. Chem. 99 (1995) 12494.
[48] M. Meot-Ner, S.G. Lias, Binding Energies Between Ions and Molecules, and The Thermochemistry of Cluster Ions in NIST Chemistry Webbook. NIST Standard Reference Database Number 69, in: P.J. Linstrom, W.G. Mallard (Eds.), June 2005, National Institute of Standards and Technology, Gaithersburg MD, 20899 (http://www.webbook.nist.gov).